

The power performance curve for engineering analysis of fuel cells

Jay B. Benziger*, M. Barclay Satterfield, Warren H.J. Hogarth,
James P. Nehlsen, Ioannis G. Kevrekidis

Department of Chemical Engineering, Princeton University, Princeton, NJ 08544-5263, USA

Received 16 March 2005; received in revised form 12 May 2005; accepted 13 May 2005
Available online 27 June 2005

Abstract

The power delivered by a fuel cell to an external load is controlled by the impedance of the external load. The power performance curve is a new metric that relates the power delivered to the external load to its impedance. The power delivered is 0 for both an open circuit and a short circuit (infinite and zero external impedance) and is a maximum when the external load impedance matches the internal resistance of the fuel cell. Fuel efficiency is 50% at maximum power output. Higher fuel efficiency is achieved when the load impedance is much greater than the internal resistance of the electrolyte. A simple equivalent circuit for the fuel cell consisting of a battery, diode and resistor captures the essential characteristics of a fuel cell as part of an electrical circuit and can be used to analyze the response to changes in load. Simple circuit analysis can be employed to elucidate the power output and efficiency of large area fuel cells and fuel cell stacks. Non-uniformities in large area fuel cells create internal potential differences that drive internal currents dissipating energy. Non-uniformities in fuel cell stacks can drive low power cells into an electrolytic state, eventually leading to failure. The power performance curve simplifies analysis of control and operation of fuel cell systems.

© 2005 Elsevier B.V. All rights reserved.

Keywords: Fuel cell; Power; Equivalent circuit; Power density; Fuel efficiency

1. Introduction

Fuel cells convert chemical energy into electrical energy. They produce an electric current through a load when connected in an electric circuit. In the hydrogen–oxygen fuel cell, hydrogen oxidation occurs at the anode producing protons and electrons. The protons move through an electrolyte to the cathode while electrons move through an external circuit. At the cathode the electrons combine with the protons and oxygen to produce water. The current and voltage depend on both the electro-chemical reaction in the fuel cell and the external load impedance. Fuel cell performance has traditionally been characterized by the voltage drop across the external load expressed as a function of the current through that load. By sweeping out a range of external loads, an IV curve (often referred to as a *polarization curve*) is obtained as shown in Fig. 1. The *polarization curve* is helpful in explaining the

chemistry and physics associated with fuel cell operation. The current is the rate of chemical reaction in the fuel cell. The voltage is the driving force for the reaction. Extensive discussion of the physical significance of the polarization curve can be found in the literature [1–6].

Different operating regimes of the fuel cell are identified with the help of the polarization curve. At open circuit (infinite external load resistance), no current flows; chemical reaction equilibrium prevails at the electrodes and the voltage is a direct measure of the difference in chemical activity of hydrogen at the anode and cathode. With a finite load resistance, current flows between the anode and the cathode; an electron current goes through the external circuit, which is balanced by an ion current going through the electrolyte. At large load resistances the voltage drops rapidly with increasing current; the steep initial decrease is attributed to the barrier for the electron transfer reactions occurring at the electrodes. This is referred to as the activation polarization region. As the load resistance is decreased further, there is a range of load resistances where the voltage decreases almost linearly

* Corresponding author. Tel.: +1 609 258 5416; fax: +1 609 258 0211.
E-mail address: benziger@princeton.edu (J.B. Benziger).

Nomenclature

A	area of electrolyte in a fuel cell element (m^2)
D_{H_2}	hydrogen diffusivity in anode gas diffusion layer ($\text{m}^2 \text{s}^{-1}$)
D_{O_2}	oxygen diffusivity in cathode gas diffusion layer ($\text{m}^2 \text{s}^{-1}$)
F	Faraday's constant, 96,500 ($\text{C}^{-1} \text{mol}$)
g	gravitational acceleration (9.8 m s^{-2})
i	current through external load (A)
i_n	current through internal fuel cell element in a parallel/series network (A)
I_0	diode saturation current (A)
k_C	mass transfer coefficient for oxygen from cathode channel to cathode surface (A bar^{-1})
k_A	mass transfer coefficient for hydrogen from anode channel to anode surface (A bar^{-1})
L	inductance of generator or motor (H)
L_A	thickness of anode gas diffusion layer (m)
L_C	thickness of cathode gas diffusion layer (m)
P	power (W)
$P_{\text{H}}^{\text{anode}}$	hydrogen pressure in the anode flow channel (bar)
$P_{\text{H}}^{\text{anode,surface}}$	hydrogen pressure at the anode surface (bar)
$P_{\text{O}}^{\text{cathode}}$	oxygen pressure in the cathode flow channel (bar)
$P_{\text{O}}^{\text{cathode,surface}}$	oxygen pressure at the cathode surface (bar)
P_{total}	total pressure in fuel cell (bar)
$P_{\text{w}}^{\text{cathode}}$	water partial pressure at cathode (bar)
P_{w}^{O}	water vapor pressure at cell temperature T (bar)
R	gas constant, $8.314 \text{ (J mol}^{-1} \text{ K}^{-1})$
R_{arm}	resistance of armature windings (Ω)
R_i	internal resistance of fuel cell element (Ω)
R_{int}	effective internal resistance of a fuel cell (Ω)
R_L	load resistance (Ω)
R_m	resistance of fuel cell electrolyte (Ω)
t	thickness of electrolyte (m)
T	fuel cell temperature (K)
v	velocity (m s^{-1})
V	voltage measured across external load (V)
V_b	fuel cell battery voltage (V)
V_n	battery voltage of a fuel cell element in a parallel/series network (V)
V_T	diode threshold voltage (V)
<i>Greek letters</i>	
θ	ramp incline
μ	dynamic coefficient of friction
ρ	electrolyte resistivity ($\Omega \text{ m}^{-1}$)
ω	frequency of revolution for generator or motor (Hz)

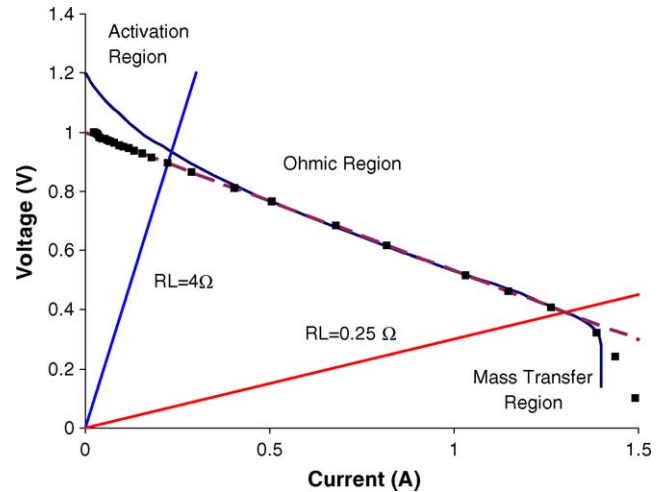


Fig. 1. A typical polarization curve for a hydrogen–oxygen polymer electrolyte membrane fuel cell. The symbols are experimental data obtained with a 1.3 cm^2 PEM fuel cell employing ETEK electrodes pressed on a Nafion™ 115 membrane. The solid line is the equivalent circuit approximation given by Eqs. (1)–(3). The three operating ranges are identified as the activation polarization region ($i < 0.2 \text{ A cm}^{-2}$), the ohmic polarization region ($0.2 \text{ A} < i < 1.25 \text{ A}$) and the mass transfer limited region ($i \sim 1.45 \text{ A}$). The polarization curve is obtained by varying the external load resistance from 0 to $\infty \Omega$. The lines radiating from the origin represent lines of constant load resistance, and indicate the range of load resistances for each of the three operating ranges. The ohmic region is approximated by a constant voltage of 1.0 V with an internal membrane resistance of 0.47Ω over the range of load resistances of $0.25\text{--}4 \Omega$ (shown by dashed line).

with the current. This is referred to as the “ohmic polarization region”, where the current is limited by the internal resistance of the electrolyte to ion flow. The ohmic region is the desirable operating regime for a fuel cell. As the external resistance is decreased further, the current reaches a limiting value where the mass transfer of reactants to the electrode/electrolyte interface limits the reaction. This is known as the concentration, or mass transfer, polarization region [7–10].

The polarization curve is useful to characterize the *chemistry and physics* of fuel cell operation; however, it does not present the *performance* of the fuel cell in the most useful form for an engineer designing a power system. We present here an alternative way to view IV performance data for a fuel cell that is more useful in designing the strategies for operation and control of a fuel cell and a fuel cell stack as part of an electrical circuit. This approach is based on systems engineering, employing the independent system parameters as the key quantities to describe and control the fuel cell.

This paper will start by defining the system parameters for a fuel cell, and then introduce the equivalent circuit for a single fuel cell. The power performance curve (PPC) for a fuel cell is introduced, which characterizes the power delivered by a fuel cell to an external load. The analysis is then extended to fuel cells in series (a stack) and in parallel (a large area fuel cell). Finally, the use of the power performance curve in defining optimal design and control strategies is discussed for both a single fuel cell and a fuel cell stack.

2. The fuel cell as part of an electric circuit

The fuel cell is the power source for an electric circuit; it is identical in function to a battery and it is appropriate to describe it as a battery. A single fuel cell, with uniform gas compositions at both the anode and the cathode, may be represented as a set of three circuit elements as shown in Fig. 2. The power source of the fuel cell is the battery voltage, V_b , resulting from the chemical potential difference across the electrolyte. The internal resistance for ion transport across the electrolyte is R_m and the activation polarization of the charge transport across the electrode/electrolyte interface may be represented by a diode with threshold voltage V_T and saturation current I_0 . The voltage and current for the hydrogen–oxygen fuel cell based on the equivalent circuit shown in Fig. 2 are given by Eqs. (1)–(3). The polarization curve shown in Fig. 1 is based on Eqs. (1)–(3) with parameters shown in Table 1. These parameters were chosen to give an approximate fit to the experimental polarization curve for a 1.5 cm² differential PEM fuel cell using ETEK electrode and a NafionTM 115 membrane [11]:

$$V_b = -\frac{\Delta G^\circ}{4F} + \frac{RT}{4F} \ln \left[\frac{(P_H^{\text{anode}} - i/2k_A)^2 (P_O^{\text{cathode}} - i/4k_C)}{(P_w^{\text{cathode}}/P_w^\circ)^2 P_{\text{total}}} \right] \quad (1)$$

$$V = V_b - V_T \ln \left[1 + \frac{i}{I_0} \right] \quad (2)$$

$$i = \frac{V}{R_m + R_L} \quad (3)$$

Eq. (1) is the thermodynamic potential of the difference of hydrogen activity at the electrode surfaces of the anode and cathode. The first term is the equilibrium potential for species at standard state. The second term is the correction for deviations away from standard state of 1 atm pressure, and for the mass transfer kinetics from the gas flow channels at the anode and cathode to the catalyst/electrolyte interface. The steady state mass balances at the electrolyte/electrode interface are given by Eq. (4); the effective reactant pressures at the electrodes ($P_O^{\text{cathode, surface}}$ and $P_H^{\text{anode, surface}}$) given in Eq. (5) are reduced from the partial pressures in the gas flow channels by the ratio of the current to the mass transfer:

$$i = 4k_C(P_O^{\text{cathode}} - P_O^{\text{cathode, surface}}) = 2k_A(P_H^{\text{anode}} - P_H^{\text{anode, surface}}) \quad (4)$$

$$P_O^{\text{cathode, surface}} = P_O^{\text{cathode}} - \frac{i}{4k_C}, \quad P_H^{\text{anode, surface}} = P_H^{\text{anode}} - \frac{i}{2k_A} \quad (5)$$

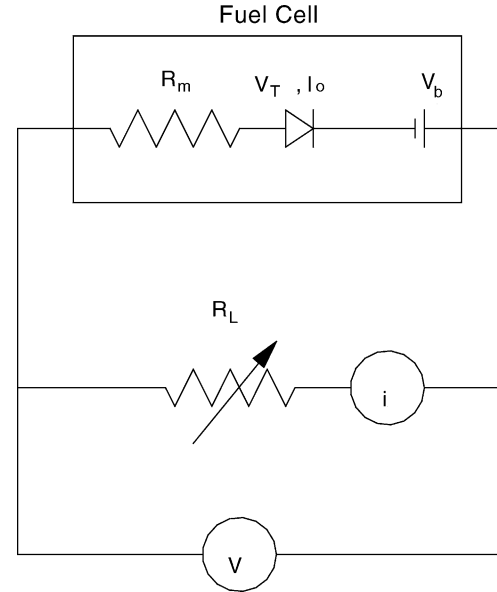


Fig. 2. Equivalent circuit for a fuel cell. The fuel cell contains the three circuit elements, the power source (battery with voltage V_b), the internal membrane electrolyte resistance for the ion (R_m), and the rectifying diode associated with the electrode polarization (defined by a saturation current I_0 and threshold voltage V_T). The external load resistance (R_L) is the manipulated parameter. The current through the load resistance (i) and the voltage across the load resistance (V) are the system variables measured.

Eqs. (2) and (3) show that the battery voltage drops across three circuit elements: the interfacial diode, the internal electrolyte resistance and the external load resistance. The load resistance can be an arbitrary load—a simple resistor, or more complex impedance (such as inductor for a motor or generator). We will restrict our analysis here to only consider steady state performance with either a simple resistive load or an ideal inductive load (representative of an ideal generator). The extension to the dynamic circuit response is straightforward, but the dynamic response must consider capacitive elements at the electrode/electrolyte interface as well as the capacitive elements in the external circuit.

The key point from the equivalent circuit model and Eqs. (1)–(3) is that the current and voltage are variables that depend on both the electrochemical reactions and the external load. It is essential to distinguish between system *parameters*,

Table 1
Fuel cell model parameters for polarization curve in Fig. 1

Parameter	Value
$\Delta G^\circ = n_e F E^\circ$ (kJ mol ⁻¹ -H ₂ O)	237
P_H^{anode} (bar)	1
P_O^{cathode} (bar)	1
$P_w^{\text{cathode}}/P_w^\circ$ (bar)	1
P_{total} (bar)	2
$k_A \sim D_{H_2}/L_A$ (A bar ⁻¹)	1.0
$k_C \sim D_{O_2}/L_C$ (A bar ⁻¹)	0.35
V_T (V)	0.15
I_0 (A)	0.08
R_m (Ω)	0.25

Table 2
Fuel cell system parameters and system variables

System parameters	System variables
Manipulated during operation	
Reactant feed flow rates	Reactant flow rates
Reactant feed composition	Reactant composition
Heat input	Cell temperature
External load resistance	Cell voltage
Pressure	Cell current
Fixed by cell design	
Electrode composition and structure	Electrolyte resistance
Electrolyte	Power
Flow field	
Electrocatalyst	

which are under the control of the operator (or control system) and system *variables* that describe the local *state* of the system.

The system variables and system parameters for a fuel cell are summarized in Table 2. The distinction between system parameters and system variables is depicted in the simplified model of a fuel cell shown in Fig. 3; system parameters are the elements outside the dashed line that can be directly controlled by the operator. (The system parameters are the actual physical knobs that are changed.) The fuel cell current and voltage are *system variables* determined by the compositional state variables at the anode and cathode and the external load resistance. Even though it is typical in an electrochemical cell to treat the current and voltage as independent variables, prescribed and controlled by an external control circuit (a galvanostat or potentiostat), *in normal fuel cell operation neither current nor voltage are independent parameters!* For engineering design and operation the external load is the independent parameter that the operator can manipulate. A simple way to see this distinction is to consider trying to arbitrarily set the current, voltage or resistance. The resistance can be set to any value and the fuel cell will function (maybe not very

well but it will always function!). However, it is impossible to guarantee that the fuel cell will function at any specified current or voltage.

The system parameters listed in Table 2 can be divided into two groups. One group of parameters is fixed by the choice of fuel cell construction, and those remain fixed unless one builds a new fuel cell. These parameters include choice of electrolyte, catalyst and flow field. The second group is the parameters that can be manipulated externally during the operation of the fuel cell reactor. These are the feed flow rates, the feed compositions, the heat input (or removal) and the external load resistance. Only the second set of parameters can be manipulated to control the performance of the fuel cell.

3. The power performance curve

When a fuel cell is connected to a circuit it becomes the power source for the external load. That load could be a light bulb, or it could be the windings of a motor as illustrated in Fig. 4. In either case power is delivered to a fixed impedance element. The fuel cell is a dc power source, like a battery. To change the current through an external load, or power delivered to an external load requires changing the resistance or impedance of the external load, or changing the voltage of the power source. Changing the voltage of a fuel cell in a controlled manner is difficult because the weak logarithmic dependence of voltage on partial pressure (see Eq. (1)). For practical applications the power output of a fuel cell is controlled by changing the load impedance. The power delivered to the external load (or useful power) is simply the product of the steady state current through the external load and voltage drop across the external load, $i \times V$; the useful power is a function of the external load impedance. The data for the polarization curve shown in Fig. 1 is re-plotted as power delivered to the external load (a *dependent system*

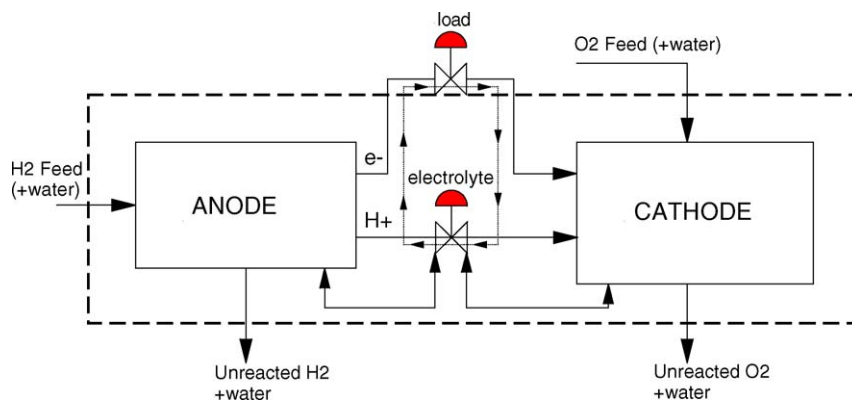


Fig. 3. Simplified model of a fuel cell reactor. The heavy dashed line represents the physical boundary for the fuel cell. The feed flows and compositions at the anode and cathode are system parameters that can be controlled. The effluents leaving the anode and cathode are system variables. The electrolyte and external load resistances regulate the current flow in the circuit shown in Fig. 2, which is indicated by the light dashed line. The light dashed line indicates that these two resistances are in series. The load resistance is external to the fuel cell boundary; it is a system parameter that can be arbitrarily varied. The electrolyte resistance is internal to the fuel cell and is a system variable that depends on water activity, temperature and other system variables.

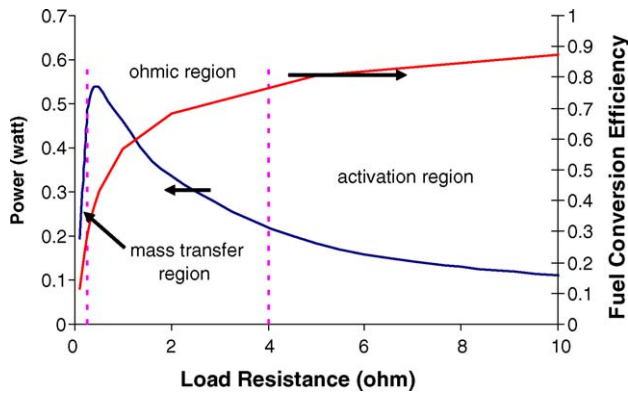


Fig. 4. Power performance curve for a single fuel cell. Parameter values are given in Table 1. The fuel conversion efficiency is shown for the same range of load resistances. The solid line replots the polarization curve shown in Fig. 1. The vertical lines divide the regions for the different polarization regimes shown in Fig. 1.

variable) as a function of the external load resistance (an independent system parameter) in Fig. 4. Fig. 4 also shows the fuel conversion efficiency of the fuel cell (the power delivered to the external load divided by the power that would be delivered to the external load if there were no internal resistances, $E = (iV)/(iV_0)$). The three operating regimes for the fuel cell operation, activation polarization, ohmic polarization and mass transfer polarization, are indicated based on the external load resistance. We refer to the plot of power as a function of external load resistance as the power performance curve (PPC).

The PPC is a useful metric to optimize fuel cells for specific applications. The key to sizing a fuel cell is to find the minimum electrode/electrolyte interface that can drive the external load resistance, such as a motor or generator as shown in Fig. 5. The power delivered to the load depends crucially on the impedance—specifying the external impedance fixes the current and voltage (and hence the power) through the external load. When the external load is fixed (such as with a light bulb, or a motor running at constant speed) the power delivered can only be changed by altering the voltage; this requires changing the partial pressures of hydrogen and oxygen at the anode and cathode by changing feed conditions. Many papers in the literature look at the power performance as a function of the current [4,9,12–17]. This is deceiving because the current delivered to a load cannot be changed without either altering the battery voltage or the external load.

The power performance curve illustrates a couple of key features about the operation of a fuel cell. Other things being kept constant, the power delivered goes through a maximum as the load resistance is varied. The maximum power occurs when the load resistance is equal to the sum of the internal resistances (the membrane resistance plus the effective diode resistance). At the maximum power output the fuel efficiency is 50%, meaning that half the energy from the fuel is dissipated internally. This has an important consequence

that is well known from automotive engineering: *fuel efficiency and power output in a fuel cell cannot be optimized simultaneously!* Fig. 4 demonstrates that, to increase the fuel efficiency, it is necessary to reduce the total power output from the fuel cell. Clearly in designing a fuel cell system one wishes to find a compromise between power density and fuel efficiency.

The maximum in power can be easily derived for a purely resistive and a purely inductive external load. Power delivered to the load is the product of the steady state current and voltage. The battery voltage from the fuel cell drops across the circuit elements in series, the electrolyte resistance, the interfacial resistance (diode resistance) and the external load impedance. The electrolyte and interfacial resistance can be combined as the internal resistance, R_{int} . The power for a resistive load is given by Eq. (6a) and the power for a purely inductive load is given by Eq. (6b). These can be differentiated to find the maximum power as a function of the resistive load, as a function of the generator's inductance at constant frequency, or as a function of the frequency of the generator at constant inductance. The maximum power for each case is given by Eq. (7):

$$P = \frac{V_b^2 R_L}{(R_{\text{int}} + R_L)^2} \quad (6a)$$

$$P = \frac{V_b^2 \omega L}{(R_{\text{int}} + \omega L)^2} \quad (6b)$$

$$P_{\text{max}} = \frac{V_b^2}{4R_L} \quad \text{at } R_L = R_{\text{int}},$$

$$P_{\text{max}} = \frac{V_b^2}{4\omega L} \quad \text{at } \omega = \frac{R_{\text{int}}}{L} \quad (\text{fixed } L)$$

$$\text{or at } L = \frac{R_{\text{int}}}{\omega} \quad (\text{fixed } \omega) \quad (7)$$

If the fuel and oxygen pressures are fixed at the anode and cathode, respectively, the power output from a fuel cell is only dependent on the external load. To illustrate how the power performance varies with the load impedance we consider a single PEM fuel cell driving a dc motor as shown in Fig. 5. The motor can be approximated as a resistor (armature resistance) and inductor in series. The current through the motor is dependent on its impedance, $Z_{\text{motor}} = R_{\text{arm}} + \omega L$. The frequency of the motor is proportional to the speed of the car; the power is the speed of the car multiplied by the frictional drag and the gravitation force.

A simple demonstration of the validity of this model was done with a model car from Thames and Kosmos [18]. The car has a PEM fuel cell driving a dc motor, as shown schematically in Fig. 5. The speed of the car, the RMS current through the motor and the RMS voltage across the motor were measured for the car going on an uphill ramp, where the ramp's slope was varied from 0° to 5° . The data from the test runs

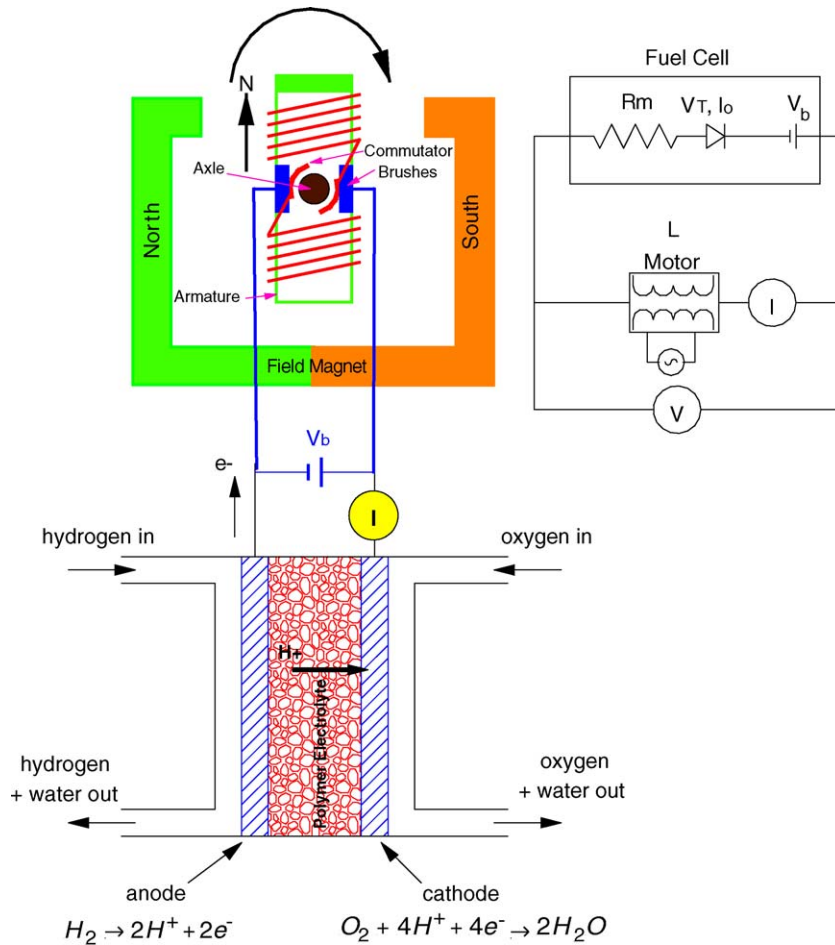


Fig. 5. Schematic of a PEM fuel cell driving a dc motor, with an equivalent circuit shown to the right. The battery voltage of the fuel cell drives the current through the external load resistance and the internal resistance of the fuel cell membrane.

are summarized in Table 3; the current, the voltage and the speed were all recorded as a function of the slope of the ramp.

The speed of the car decreased as the slope of the ramp increased. The voltage decreased and the current increased as the speed of the car decreased. These trends fit the equivalent circuit model with the motor represented as an inductor. The model's expressions for current and voltage through a resistor in series with a fixed inductor are given by Eq. (8). Gravity slows down the car so that ω decreases, which results in the voltage decreasing and the current increasing from lower motor impedance:

$$V = \frac{V_b R_{arm} - \omega L R_{int}}{R_{int} + R_{arm}}, \quad i = \frac{V_b - \omega L}{R_{int} + R_{arm}} \quad (8)$$

The power delivered by the fuel cell to the motor is given by the current through the circuit multiplied by the voltage drop across the motor. The motive power to move the car up the ramp at angle θ is given by Eq. (9):

$$\begin{aligned} \text{motive power} &= (\mu mg + mg \sin \theta)v \\ &= (\mu mg + mg \sin \theta)\omega r_{\text{wheel}} \end{aligned} \quad (9)$$

The car mass was 325 g. A dynamic coefficient of friction for the car of 0.2 was estimated from rolling the car down an inclined plane. The computed electrical power and the motive power as functions of the car's measured speed are plotted in Fig. 6. As predicted by the model there is an optimal electrical power output and an optimal motive power as a function of

Table 3
Fuel cell car performance

Ramp inclination (°)	Car speed (m s ⁻¹)	Current (A)	Voltage across motor (V)	Power delivered to motor (W)
0	0.240	0.253	0.730	0.185
1.5	0.216	0.291	0.700	0.204
3.1	0.200	0.385	0.680	0.262
4.6	0.125	0.480	0.646	0.310

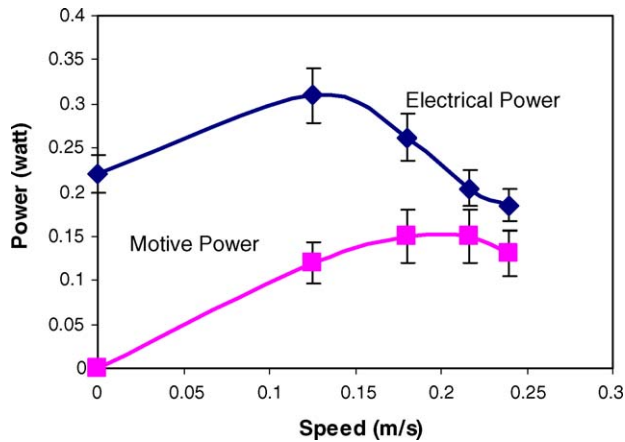


Fig. 6. Performance of a fuel cell powered model car. A single PEM fuel cell powers a dc motor that propels the car up a ramp. The power to the wheels (motive power = $(\mu mg + mg \sin \theta)v$) and the electrical power dissipated by the motor (electrical power = iV) were determined as a function of speed going up a ramp at different inclinations. The trend lines shown are simple spline fits.

the car speed. The maximum electrical power dissipated in the motor does not occur at the same speed as the maximum motive power delivered to the wheels. These occur at different speeds because of the resistance of the armature windings, so that even at zero speed there is power dissipation in the motor.

These results are only semi-quantitative. The partial pressures at the electrodes are not controlled, and the friction losses on the motor and drive train are substantial. But the results clearly show how the PPC can be useful to match the external impedance with the internal impedance of the fuel cell to achieve maximum power output.

The power performance curve shown in Fig. 4 gives a clear representation of the power delivered by the fuel cell as a function of the control parameter, the load resistance. Often the power is reported as a function of current instead. This

representation of performance can be misleading, because current is not an independent parameter. To change the current delivered to the motor shown in Fig. 4, either the load impedance must be changed or the fuel feed must be changed to change the voltage. Changes to either the external load or the fuel feed will alter both the battery voltage and the current delivered by the fuel cell. It is impossible to change the current or voltage without changing one of the manipulated parameters.

4. Strategies for controlling power delivery

The power performance curve shows that the power delivered takes a unique value based on the *load impedance*. There are two obvious ways to manipulate the power delivered to a load. Varying the gas phase compositions at the anode and cathode can be used to adjust the battery voltage and hence the power delivery. However, the battery voltage is not very sensitive to changes in the gas phase composition; the battery voltage varies logarithmically with partial pressure, changing the anode hydrogen partial pressure ten-fold will only change the voltage by ~ 50 mV. The feed to the fuel cell should be altered to maintain good fuel utilization, but changing the fuel feed to alter the power output from a fuel cell will not be very effective. Changing the external load impedance is a more effective method to alter the power delivery. Additional load resistances can be added in parallel or in series with the motor to achieve different objectives for power output and efficiency. Fig. 7 shows how the power changes when a resistor is placed in parallel or in series relative to the base load. The current, total power, power in the base load, and overall fuel efficiency for this arrangement is shown in Table 4. When the control resistor is placed in series with the base load both the total power delivered by the fuel cell and the power to the base load decrease, while

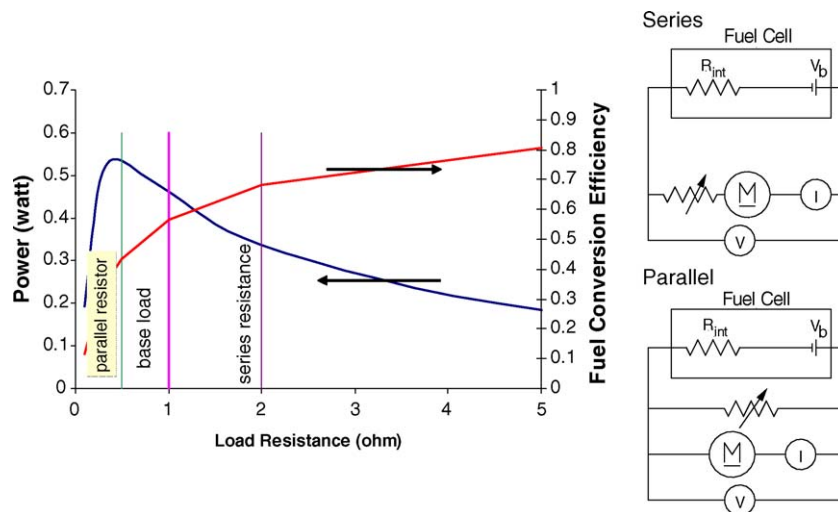


Fig. 7. Strategies for controlling the power delivered by a fuel cell. A 1Ω resistor is placed either parallel to or in series with a 1Ω load. The fuel cell representation has been simplified to include the diode as part of the internal resistance of the fuel cell.

Table 4
Effect of added loads to base load power

Circuit	Fuel cell current (A)	Total power delivered by fuel cell (W)	Total power to base load (W)	Overall fuel efficiency (%)
1 Ω base load	0.68	0.46	0.46	57
1 Ω base load + 1 Ω resistance in series	0.41	0.34	0.17	68
1 Ω base load + 1 Ω resistance in parallel	1.04	0.53	0.28	43

the overall fuel efficiency increases. Alternatively, when the control resistance is placed in parallel to the base load the overall power delivered from the fuel cell increases while power to base load and the fuel efficiency both decrease.

To achieve good fuel efficiency and power output, it is most effective to run the fuel cell with a *constant load* where the impedance is matched to the fuel cell's internal resistance. It is necessary to provide for a power conditioning system to drive a motor or generator at variable power output. Ideally the fuel cell would be part of a hybrid system where it would operate a generator at steady power. Matching the generator impedance to the internal resistance of the fuel cell would permit the designer to achieve high fuel efficiency and high power output. To vary the power delivered by the power system a secondary system (e.g. batteries) would supplement the power generated by the fuel cell. Battery power would supplement the fuel cell when the power demand exceeded the power delivered by the generator, and the battery would be recharged when the demand was less than the generator output. Hybrid strategies have been built and discussed in the literature [19–23]. The power performance curve provides guidance to optimize the fuel cell in a hybrid system.

The hybrid system is shown schematically in Fig. 8. In developing the hybrid system the design engineer must choose between different options, which are similar to those for an internal combustion engine/battery system. Two obvious options are:

- (1) A fuel cell that always operates at steady state with a fixed resistive load. The output power from the fuel

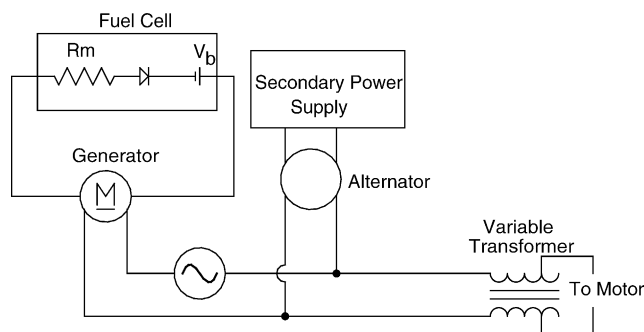


Fig. 8. Fuel cell hybrid system. The fuel cell is designed to drive a generator at constant load. The power from the generator is connected to a secondary power system via an alternator that supplements the output from the generator or recharges the batteries in the secondary power system.

cell is constant, and a secondary power system (batteries) is constantly being charged or discharged to match changing load demand. The fuel cell should be designed for its base load to achieve the optimal choice of power density and fuel efficiency based on matched impedance.

- (2) A fuel cell that operates with a variable load and a secondary power system. The variable load permits higher sustained power from the fuel cell reducing the size requirement for the secondary power system. The variable load can be added as a parallel or series resistance to achieve increased power output or increased fuel efficiency.

The concept of improving fuel efficiency with fuel cell and battery systems has been advocated by a number of power systems engineers [19,20]. Hybrid systems permit a reduction in size of the primary power source and they permit the use of power sources with different voltages. The power performance curve analysis has identified the importance of impedance matching to optimize the power density or fuel efficiency from a fuel cell, which are key elements to an efficient hybrid system.

5. Large area fuel cells

Fuel cells for power systems and automobiles have a large electrode/electrolyte interface; reactants flow through long flow channels delivering the reactant gases and carrying away the product water. Variations in the gas phase composition along the flow channels and variations in the membrane water content give rise to non-uniform current densities, local potential and electrolyte resistivity. The analysis of large area fuel cells can be simplified by representing the large cell by a set of smaller cells in parallel; Fig. 9 shows three cells in parallel, but that number can be increased to more accurately capture the compositional variations. Local compositional differences are represented as differences in the battery voltages and internal resistances of the individual elements. Hydrogen consumption in a hydrogen–oxygen fuel cell decreases the local voltage (battery voltage) along the length of a flow channel. Variations of the local water concentration will change the local resistivity of the electrolyte membrane in PEM fuel cells. Temperature variations will alter the local electrolyte resistivity in solid oxide fuel cells (SOFC).

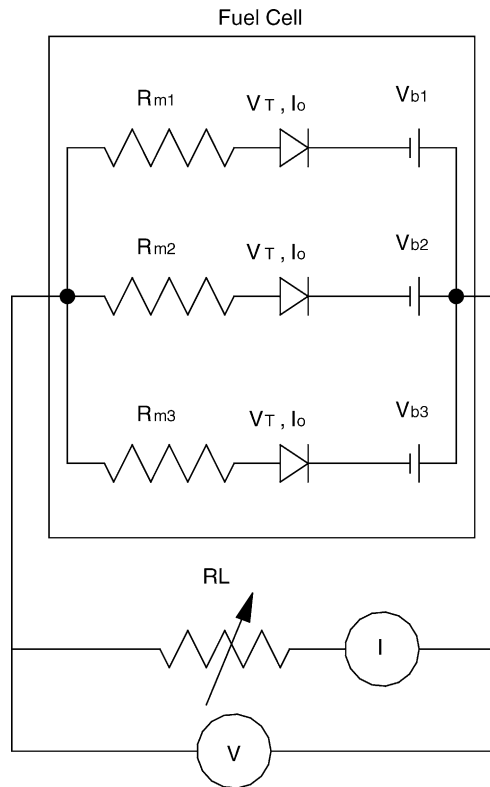


Fig. 9. Equivalent circuit for a three-element fuel cell approximation of a large area fuel cell. The local battery voltages, $V_{b1} - V_{b3}$, depend on local compositions at the anode and cathode as given by Eq. (1). The local resistance depends on the local composition and temperature. Local current densities can be determined from solving Kirchhoff's law with the external load resistance, R_L , specified.

The discrete cell model employed here to model large area fuel cells sacrifices some accuracy of the 2D and 3D differential models found in the literature [24–28]. However, the discrete model provides a simpler physical model that can assist engineers in preliminary examination of different designs; it is especially helpful in analyzing the effect of the external load impedance. The local current density of a large area fuel cell is mapped onto the current through the corresponding resistor of the network of parallel resistors representing the electrolyte. The external load resistance is still the system parameter that controls the total current, and hence all the local currents. The overall fuel cell current and voltage can be determined by employing Kirchhoff's law to reduce the network of parallel batteries and resistors to an “effective fuel cell voltage” and an “effective electrolyte resistance”.

The parallel network of discrete elements for the large area fuel cell provides a simple way to understand some of the inefficiencies. The local current density is greatest in the element with the lowest internal resistance; this is equivalent to saying the local current density is highest where the local ionic conductivity is greatest. The overall voltage is a weighted average of the local battery voltages in each element.

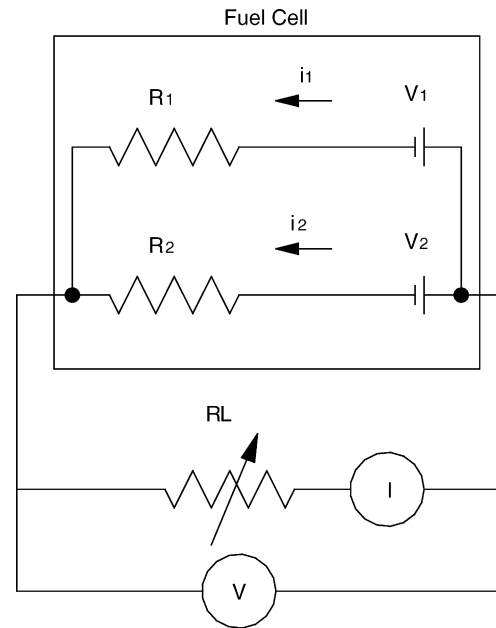


Fig. 10. Simplified two cells in parallel. When the two local voltages, V_1 and V_2 , are not equal an internal current is driven in the fuel cell, which dissipates power internally to the fuel cell diminishing the power output and fuel efficiency of the fuel cell.

The parallel cell model reveals that potential differences across the fuel cell can drive internal currents that diminish the overall power output from the fuel cell. Non-uniform electrolyte resistance in the fuel cell creates non-uniform current distributions that also diminish the power output and efficiency in fuel cells. These phenomena can be illustrated with a simplified model of two cells in parallel as shown in Fig. 10. The diodes have been left out of the circuit for simplicity. If the fuel cell had uniform composition at both the anode and cathode, and the electrolyte had uniform conductivity the voltages and the resistances in both cells would be the same, $V_1 = V_2$ and $R_1 = R_2 = \rho(A/2)/t$, where the voltage would be given by Eq. (1), ρ is the electrolyte resistivity, A is the electrode/electrolyte interfacial area and t is the electrolyte thickness. The voltage drop across the external load resistance is $V = V_1 R_L / (R_1/2 + R_L)$ and the power delivered to the external load resistance is $P = V^2 / (R_1/2 + R_L)$.

Consider two deviations from the uniform fuel cell.

- (1) The case where the electrolyte resistance is the same in both cells, but the voltages are different due to compositional differences between the inlet and outlet of the fuel cell, then $R_1 = R_2$ and $V_1 > V_2$.
- (2) The case where the electrolyte resistance is different in the two cells, but the voltages are the same, then $R_1 \neq R_2$ and $V_1 = V_2$.

In case 1, a current is driven between the high potential cell and the low potential cell. The voltage across the external load resistance is an averaged value between the potential in

the two cells in parallel:

$$V = \frac{(V_1 + V_2)R_L}{(R_1 + 2R_L)} \quad (10)$$

The power delivered to the external load resistance decreases as the voltage difference between the two cells increases; the power relative to the base case is given by Eq. (11):

$$\frac{(\text{Power})_I}{(\text{Power})_0} = \frac{(V_1 + V_2)^2}{4V_1^2} \quad (11)$$

This decrease in power to the external load resistance is accompanied by an internal current generated between the high and low potential elements. This internal current, Δi depends on the potential difference, the electrolyte resistance and the external load resistance. For the simplified model shown in Fig. 10 the internally generated current is given by Eq. (12). This internal current dissipates energy and reduces the useful power output:

$$\Delta i = i_1 - i_{1,0} = \frac{(V_1 - V_2)R_L}{R_1(R_1 + R_L)} \quad (12)$$

The second case considered is when the voltage is uniform but the electrolyte resistance is not uniform in the elements. The current will flow through the path of least resistance, giving rise to higher currents in the low resistance elements. The non-uniform currents result in a decrease in the voltage across the external load resistance and reduce the power delivered to the external load. The power delivered to the external load is given by Eq. (13):

$$P = \frac{V_1^2(R_1 + R_2)^2 R_L}{(R_1 R_2 + (R_1 + R_2)R_L)^2} \quad (13)$$

The power performance curve for elements in parallel depends on the ratio of the resistances in the two elements, $\alpha = R_2/R_1$, for uniform voltage. Fig. 11 shows the Power Performance Curves as a function of α ; the power output decreases for all load resistances, but the power density falls

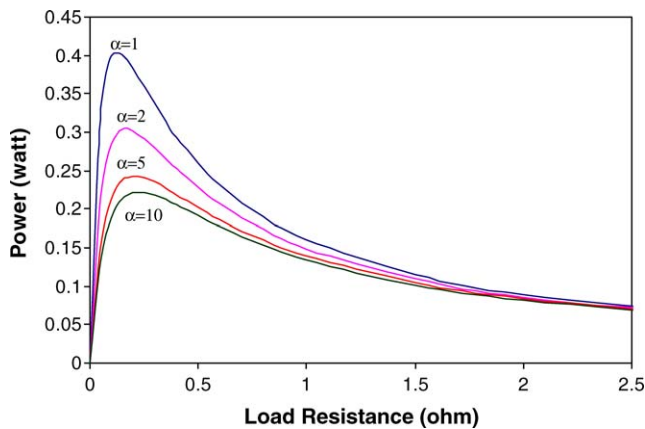


Fig. 11. Power performance curves for two fuel cell elements in parallel. The curves are presented for $V_1 = 0.9$ V, $R_1 = 0.25$ Ω and values of $\alpha = R_2/R_1$ from 1 to 10.

by 50% when a fuel cell is operating near the maximum power density.

This simple model illustrates how critically dependent the power output from a large area fuel cell is on the compositional variations in both fuel and membrane water content. Any large area fuel cell can be represented by the simple equivalent circuit shown in Fig. 2, where the effective voltage, internal resistance, diode threshold voltage and saturation current are determined from a simple circuit reduction. The critical result is that the power output is determined by the external load impedance; power density is maximized when the external load impedance matches the internal fuel cell impedance.

An advantage of a large area fuel cell is that the effective overall electrolyte resistance decreases with increasing area, so the internal resistance is small; when powering moderate load impedances with large area cells the overall fuel efficiency will be satisfactory. However, micro or miniature fuel cells could struggle with efficiency if the system is not well designed. When the electrode/electrolyte interfacial area is small, the internal resistance will be large. If the circuit elements being powered by the micro fuel cell have lower resistance than the electrolyte resistance, the fuel efficiency will be very poor (<50%). It is critical to make sure the load impedances are properly matched with the fuel cell impedance! The connection between fuel cell performance and the external load is critical to make in design and control. The fuel cell literature focuses on the intensive property of current density [1–6,8,26]. However, the current (and current density) are system variables that are dependent on the system external load resistance, which is an extensive property.

6. Fuel cell stacks

Any single fuel cell can be represented as a battery–diode–resistor combination. The system parameters that control the current/voltage relationship and the power output are the feed compositions and flow rates to the anode and cathode and the external load resistance. A fuel cell stack can be modeled as a series of the battery–diode–resistor elements for a single fuel cell, as shown in Fig. 12 for a simple three-cell stack.

The cells in series can be reduced using simple application of Kirchhoff’s law to determine effective voltages and resistances for the stack. The battery voltage in each cell is determined by the compositions at the anode and cathode in each cell through the use of Eq. (1). The overall voltage and current across the external load is then given by Eqs. (14) and (15):

$$V = \sum_{\text{cells}} V_{b,i} - \sum V_{T,i} \ln \left(1 + \frac{i}{I_{0,i}} \right) \quad (14)$$

$$i = \frac{V}{\sum_{\text{cells}} R_{m,i} + R_L} \quad (15)$$

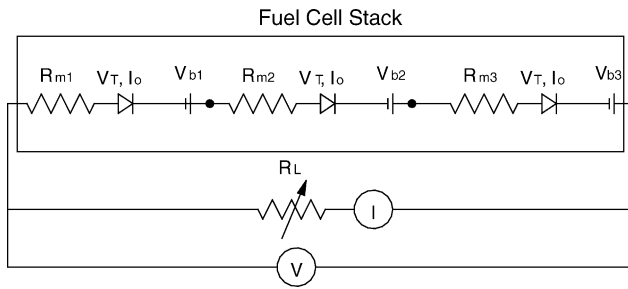


Fig. 12. Equivalent circuit model of a three-cell stack. Each cell is represented by a battery–diode–resistor combination. The external load resistance is connected across the stack with the current measured through the load resistance and the voltage measured across the load resistance.

The power performance curve for a fuel cell stack looks just like that for a single cell as shown in Fig. 4, with the only difference being that the total power output scales with the number of cells and the maximum power output occurs when the internal resistance of the stack matches the external load impedance. If all the cells in the stack were identical the maximum power output would be nP , where n is the number of cells in the stack and P is the maximum power from a single cell. For a purely resistive load the maximum power would occur at an external load resistance $R_L = nR_{int}$, where R_{int} is the internal load resistance of a single cell (the combined resistance of the electrolyte and the interfacial resistance of the diode circuit element). For a fuel cell stack the maximum power density occurs when the external and internal resistances are matched, and the fuel efficiency is 50% at maximum power density.

The current in a fuel cell stack is the same in each cell; to maintain the same current in each cell, the voltage across each cell must adjust to compensate for differences in the battery voltages of each cell and the internal resistances in each cell. The voltage across each cell, V_n , is given by Eq. (15):

$$V_n = V_{b,n} - V_{T,n} \ln \left(1 + \frac{i}{I_{0,n}} \right) - iR_{m,n} \quad (16)$$

In a perfectly matched stack the voltage across each cell is the same, and the internal power dissipation in each cell is the same. However, when the cells in a stack are not matched the cells with greater power output capacity (those cells having the lowest internal resistance or highest battery voltage) will drive cells with lower capacity. The mismatch between cells can result from three causes:

- (1) The electrolyte resistances of different cells are different. This could occur in a PEM fuel cell when the water content in different cells causes different membrane conductivities. In an SOFC, different temperatures could result in different conductivities. This is reflected by $R_{m,n}$ having different values in the stack.

- (2) The interfacial resistances may be different between different cells. This can occur due to catalyst poisoning altering the threshold voltage, V_T . It can also result from differences in the electrolyte/electrode interfacial contact, from delamination or other causes, which would alter the diode saturation current $I_{0,n}$.
- (3) The battery voltage may change from cell to cell. This can result from different flow rates to each cell causing different compositions, or in PEM fuel cell it could result from flooding. The result of the different battery voltages between cells is differences in $V_{b,n}$.

When fuel cells in a stack are mismatched the differences in the voltage across each cell can become large when the external load impedance is reduced. Since the current is the same in every cell in the stack, cells with higher power output (i.e. those cells having low internal resistance or high battery voltage) will drive low power output cells. In a large stack it is possible for low power cells to build up a negative cell voltage (i.e. $V_n < 0$), and become electrolytic cells, where water is oxidized. Oxygen formed at the anode by water oxidation can attack the electrolyte/electrode interface ultimately leading to anode failure. This can be illustrated with a simple stack of five cells in a PEM stack driving a 0.5Ω load. We assume the feed to each cell is identical so the battery voltage in each cell is 1 V. Suppose the center cell (cell 3) in the stack is at a higher temperature so the membrane is partially dried out. Cells 1, 2, 4 and 5 each have an internal resistance of 0.25Ω and cell 3 has a resistance of 1Ω . The current through the stack is 2.5 A ($\Sigma V/R_L + \Sigma R = 5 \text{ V}/2.5 \Omega = 2 \text{ A}$). The individual cell voltages are the battery voltage minus the IR voltage drop. The voltage drop across each cell in the stack and the power dissipated in each cell is listed in Table 5. The current has driven cell 3 into an electrolytic state. Furthermore, the power dissipated in cell 3 is much greater than in the other four cells; if the heat exchanger system treats every cell equivalently the temperature in cell 3 will rise due to insufficient heat removal and the situation will be exacerbated. Driving cell 3 into an electrolytic state is clearly a problem that should be avoided. The positive feedback associated with the high power dissipation will continue to dry the membrane out until the resistance of the cell becomes so large to make the stack fail. Two control schemes could alleviate this problem, both of which depend on monitoring the individual cell voltages. If the cooling to each cell was controlled in response to the cell voltage it would be possible to bring the offending cell into compliance and avoid the problem. Alternatively, a shunt resistance could be placed in parallel with each cell and the

Table 5
Voltage and power distribution in a PEM fuel cell stack

Cell	1	2	3	4	5
Battery voltage, V_b (V)	1.0	1.0	1.0	1.0	1.0
Internal resistance, R_m (Ω)	0.25	0.25	1.0	0.25	0.25
Cell voltage (V)	0.5	0.5	–1.0	0.5	0.5
Internal power dissipation (W)	1.0	1.0	4.0	1.0	1.0

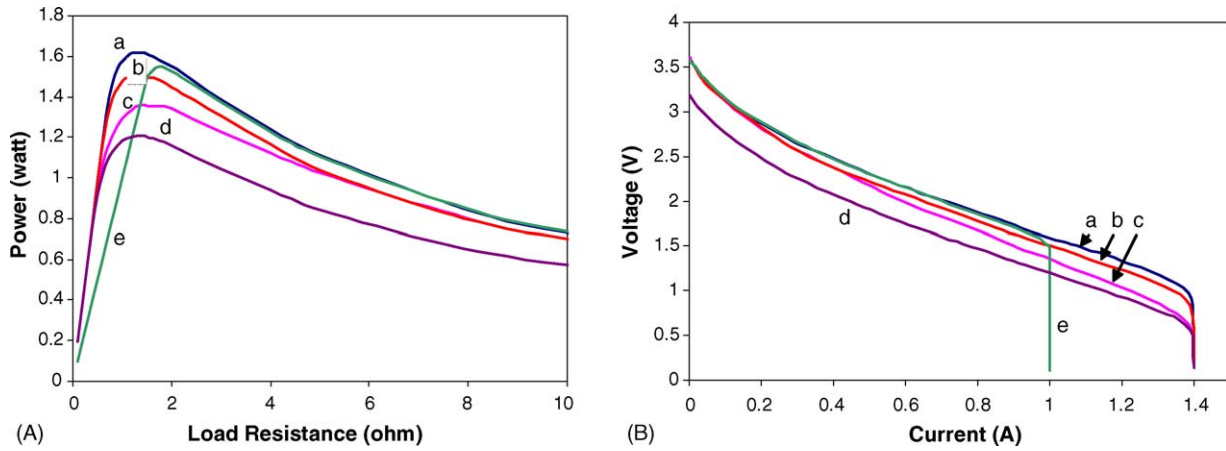


Fig. 13. (A) Power performance curves for a three-cell stack showing the effects of mismatched cells. The parameters for the fuel cells are listed in Table 6. (B) IV Curves for a three-cell stack showing the effects of mismatched cells. The parameters for the fuel cells are listed in Table 6.

Table 6
Fuel cell parameters in three-cell stack

	Cell 1					Cells 2 and 3				
	<i>a</i>	<i>b</i>	<i>c</i>	<i>d</i>	<i>e</i>	<i>a</i>	<i>b</i>	<i>c</i>	<i>d</i>	<i>e</i>
V_0 (V)	1.2	1.2	1.2	0.8	1.2	1.2	1.2	1.2	1.2	1.2
V_T (V)	0.15	0.15	0.15	0.15	0.15	0.15	0.15	0.15	0.15	0.15
I_0 (A)	0.08	0.04	0.08	0.08	0.08	0.08	0.08	0.08	0.08	0.08
R_m (Ω)	0.25	0.25	0.50	0.25	0.25	0.25	0.25	0.25	0.25	0.25
$p_{O}^{cathode}$ (bar)	1	1	1	1	1	1	1	1	1	1
k_C ($A\ bar^{-1}$)	0.35	0.35	0.35	0.35	0.25	0.35	0.35	0.35	0.35	0.35

shunt resistance could be controlled to keep all the cell voltages the same.

To further illustrate the effects of mismatched cell conditions on a PEM stack performance we modeled the effects of membrane resistance (R_m), battery voltage (V_b), electrolyte/electrode interfacial voltage (V_T), electrolyte/electrode interfacial contact area (I_0) and mass transfer across the gas diffusion layer (k_C) on both the power performance curve and the IV curve for the stack. The results are shown in Fig. 13; the parameters for the different curves are listed in Table 6. Curve a is the base case of three perfectly matched cells and the other four curves show the changes when a single parameter was changed in one cell: the electrolyte resistance (curve b), the electrolyte/electrode interface (curve c), the open circuit potential (curve d) and the oxygen mass transfer coefficient at the cathode (curve e).

Fig. 13 reveals that any mismatch in the fuel cell characteristics of a single cell will degrade the power output from the stack. However, the source of the mismatch produces different power reduction as a function of the external load resistance. Both a higher electrolyte resistance (curve c) and decreased interfacial area (curve b) produce similar results, where the maximum power is decreased but the power output approaches the matched network at high loads. If the stack is being operated for high fuel efficiency and not for high

power density, this is not a significant problem. When the open circuit voltage is reduced, from fuel crossover across the electrolyte, the maximum power output is decreased and the power is less at all load resistances (curve d). When the mass transfer resistance at the cathode increases, the power output is dramatically reduced at low load resistances, but is unchanged at high load resistances (curve e). These different responses should be considered in choosing control systems for fuel cell stacks.

Simulations of PEM fuel cell stacks have found that unequal distribution of the reactants among cells degrades performance [27,29–31]. The power performance analysis presented here provides a simple systematic explanation of those observations, and illustrates the importance of impedance matching to achieve the optimal performance from individual cells and stacks of cells.

7. Conclusions

The essential point presented in this paper is that the power delivered by a fuel cell and the fuel efficiency are critically dependent on the external load being driven, and maximum power density and fuel efficiency cannot be achieved simultaneously. The external load is the independent system param-

eter that can be controlled to change the power delivered by a fuel cell or a fuel cell stack. Neither current nor voltage are independent variables in fuel cell operation and the analysis of fuel cell operation assuming they are independent variables can be misleading. A simple equivalent circuit representation of a fuel cell composed of a battery, diode and resistor captures the essential operational characteristics of a fuel cell as part of an electrical circuit. Employing this equivalent circuit permits easy conceptual analysis of how the fuel cell responds to changes in external load.

A new construct of fuel cell performance called the power performance curve was introduced. This performance curve plots power delivered as a function of the manipulated parameter, the external impedance. The PPC shows that the power is maximized when the external load impedance is matched to the internal resistance of the fuel cell system. At the maximum power output the fuel efficiency is only 50%. When the external load impedance exceeds the internal impedance (in the “ohmic” polarization region) the power output decreases with increasing load resistance, but fuel efficiency increases. Strategies for fuel cell systems are better understood using the power performance curve. It is shown that for a motor or generator there is an optimal frequency for the power output.

Power delivered by the fuel cell is maximized when the external load matches the internal resistance of the fuel cell system. It is not possible to maximize both power density for a fuel cell system and the fuel efficiency; the fuel efficiency of a fuel cell is only 50% when power density is maximized. Fuel efficiency increases as the ratio of the external load to the internal resistance increases, but total power output decreases.

The power performance of large area fuel cells or fuel cell stacks is diminished by non-uniformities. In large area fuel cells, variable voltages due to compositional variations can create internal currents that dissipate energy. In fuel cell stacks, differences in voltages or internal resistances between cells can cause negative voltages to build up across high resistance cells which can drive cells into an electrolytic state detrimental to overall stack operation.

We believe the power performance curve provides a useful engineering perspective on fuel cell operation that focuses on the key system variable (power) as a function of the key system parameter (load impedance).

Acknowledgements

The authors thank the National Science Foundation (CTS-0354279 and DMR-0213707 through the Materials Research and Science Engineering Center at Princeton) and the Air Force Office of Scientific Research (Dynamics and Control) for their support of this work. W.H.J.H. thanks the Australian-American Fulbright Commission for fellowship support and the ARC Centre for Functional Nanomaterials at the University of Queensland.

References

- [1] EG&G Services I. Parson, Fuel Cell Handbook, U.S. Department of Energy, Morgantown, WV, 2000.
- [2] L.J.M. Blomen, M.Ne. Mugerwa, Fuel Cell Systems, Plenum Press, New York, 1993.
- [3] J.O.M. Bokris, S. Srinivasan, Fuel Cells: Their Electrochemistry, McGraw Hill, New York, 1969.
- [4] L. Carrette, K.A. Friedrich, U. Stimming, Fuel cells: principles, types, fuels, and applications, *Chemphyschem* 1 (4) (2000) 162–193.
- [5] S. Srinivasan, et al., in: L.J.M.J. in Fuel Cell Systems, M.N. Blomen, Mugerwa (Eds.), Overview of Fuel Cell Technology, Plenum Press, New York, 1993, pp. 37–72.
- [6] A.Z. Weber, J. Newman, Modeling transport in polymer-electrolyte fuel cells, *Chem. Rev.* 104 (10) (2004) 4679–4726.
- [7] D.M. Bernardi, M.W. Verbrugge, A mathematical-model of the solid-polymer-electrolyte fuel-cell, *J. Electrochem. Soc.* 139 (9) (1992) 2477–2491.
- [8] C.Y. Wang, Fundamental models for fuel cell engineering, *Chem. Rev.* 104 (10) (2004) 4727–4765.
- [9] Z.H. Wang, C.Y. Wang, K.S. Chen, Two-phase flow and transport in the air cathode of proton exchange membrane fuel cells, *J. Power Sources* 94 (1) (2001) 40–50.
- [10] U. Pasaogullari, C.Y. Wang, Two-phase modeling and flooding prediction of polymer electrolyte fuel cells, *J. Electrochem. Soc.* 152 (2) (2005) A380–A390.
- [11] J.B. Benziger, et al., A differential reactor polymer electrolyte membrane fuel cell, *AIChE J.* 50 (8) (2000) 1889–1900.
- [12] J.J. Baschuk, X.H. Li, Modelling of polymer electrolyte membrane fuel cells with variable degrees of water flooding, *J. Power Sources* 86 (1/2) (2000) 181–196.
- [13] A. Kazim, H.T. Liu, P. Forges, Modelling of performance of PEM fuel cells with conventional and interdigitated flow fields, *J. Appl. Electrochem.* 29 (12) (1999) 1409–1416.
- [14] R.F. Mann, et al., Development and application of a generalised steady-state electrochemical model for a PEM fuel cell, *J. Power Sources* 86 (1/2) (2000) 173–180.
- [15] T.E. Springer, et al., Model for polymer electrolyte fuel cell operation on reformate feed—effects of CO, H₂ dilution, and high fuel utilization, *J. Electrochem. Soc.* 148 (1) (2001) A11–A23.
- [16] S. Srinivasan, et al., High energy efficiency and high power density proton exchange membrane fuel cells – electrode kinetics and mass transport, *J. Power Sources* 36 (1991) 299–320.
- [17] T. Thampan, et al., PEM fuel cell as a membrane reactor., *Catal. Today* 67 (1–3) (2001) 15–32.
- [18] Thames, Kosmos, Fuel Cell Car (2002).
- [19] R.K. Ahluwalia, X. Wang, Direct hydrogen fuel cell systems for hybrid vehicles, *J. Power Sources* 139 (1/2) (2005) 152–164.
- [20] M.J. Blackwelder, R.A. Dougal, Power coordination in a fuel cell-battery hybrid power source using commercial power controller circuits, *J. Power Sources* 134 (1) (2004) 139–147.
- [21] Z.H. Jiang, L.J. Gao, R.A. Dougal, Flexible multiobjective control of power converter in active hybrid fuel cell/battery power sources, *IEEE Trans. Power Electron.* 20 (1) (2005) 244–253.
- [22] C. Park, et al., Development of fuel cell hybrid electric vehicle performance simulator, *Int. J. Automotive Technol.* 5 (4) (2004) 287–295.
- [23] H.P. Xu, L. Kong, X.H. Wen, Fuel cell power system and high power dc-dc converter, *IEEE Trans. Power Electron.* 19 (5) (2004) 1250–1255.
- [24] T. Berning, D.M. Lu, N. Djilali, Three-dimensional computational analysis of transport phenomena in a PEM fuel cell, *J. Power Sources* 106 (1/2) (2002) 284–294.
- [25] W.S. He, J.S. Yi, T. Van Nguyen, Two-phase flow model of the cathode of PEM fuel cells using interdigitated flow fields, *AIChE J.* 46 (10) (2000) 2053–2064.

- [26] A.Z. Weber, R.M. Darling, J. Newman, Modeling two-phase behavior in PEFCs, *J. Electrochem. Soc.* 151 (10) (2004) A1715–A1727.
- [27] J.J. Baschuk, X.G. Li, Modelling of polymer electrolyte membrane fuel cell stacks based on a hydraulic network approach, *Int. J. Energy Res.* 28 (8) (2004) 697–724.
- [28] J. Mantzaras, et al., Fuel cell modeling and simulations, *Chimia* 58 (12) (2004) 857–868.
- [29] J.M. Correa, et al., An electrochemical-based fuel-cell model suitable for electrical engineering automation approach, *IEEE Trans. Ind. Electron.* 51 (5) (2004) 1103–1112.
- [30] J.H. Lee, T.R. Lalk, Modeling fuel cell stack systems, *J. Power Sources* 73 (2) (1998) 229–241.
- [31] W.Y. Lee, et al., Empirical modeling of polymer electrolyte membrane fuel cell performance using artificial neural networks, *Int. J. Hydrogen Energy* 29 (9) (2004) 961–966.